Electronic Supplementary Material (ESI) for Analyst.

Supporting information

Lipid-conjugated fluorescent pH sensors for monitoring pH changes in reconstituted membrane systems

Gerdi Christine Kemmer[a], Sidsel Ammitzbøll Bogh[b], Michael Urban[c], Michael G. Palmgren[a], Tom Vosch[b], Jürgen Schiller[d], Thomas Günther Pomorski[a,*]

[a] Centre for Membrane Pumps in Cells and Disease – PUMPKIN, Department of Plant Biology and Biotechnology, University of Copenhagen, Thorvaldsensvej 40, 1871 Frederiksberg C, Denmark
[b] Nano-Science Center, Department of Chemistry, University of Copenhagen, Universitetsparken 5, 2100 Copenhagen, Denmark
[c] Institute of Biochemistry, Biocenter, Goethe-University, Max-von-Laue-Str. 9, D-60438 Frankfurt, Germany
[d] Institute of Medical Physics and Biophysics, Faculty of Medicine, University of Leipzig, 04107 Leipzig, Germany

List of contents

1. Scheme of SNARF conjugation to DOPE

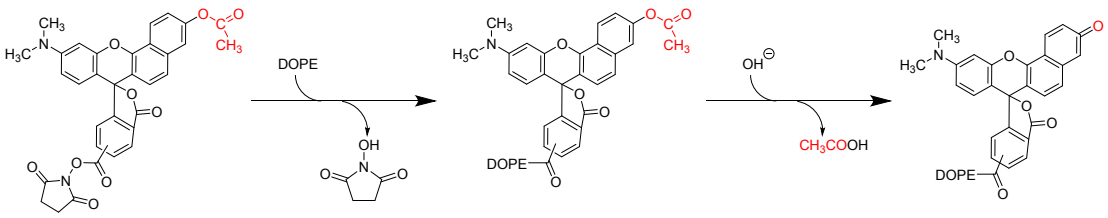

Figure S1: SNARF conjugation to DOPE. SNARF®-1 carboxylic acid acetate succinimidyl ester reacts with the amino-group of DOPE via a nucleophilic attack. The aryl acetyl group (shown in red) is removed under alkaline conditions, yielding SNARF-DOPE.

2. Lipid head group composition of lecithin

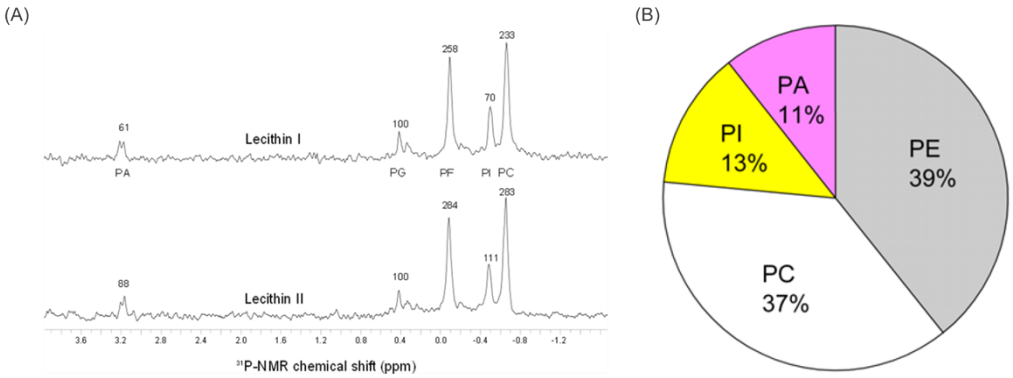

Figure S2: Lipid head group composition of lecithin. Two different batches of lecithin were subjected to ^{31}P-NMR-analysis (A), integrated intensities normalized to 100%, and the average of both batches used to plot as a pie chart (B). Before analysis, lipids were solubilized in 200 mM sodium cholate, 5 mM EDTA in D_2O. ^{31}P NMR spectra were recorded on a Bruker DRX-600 spectrometer operating at 242.94 MHz. All measurements were performed on 0.6 ml samples in 5 mm NMR tubes using a 5 mm ‘‘direct’’ broadband probe at 37uC. Composite pulse decoupling (Waltz-16) was applied to eliminate 31P-1H coupling. Other NMR parameters were as follows: Data size: 16 k, 60° pulse (5 µs), pulse delay 2 s. A line broadening of 2 Hz was applied for the processing of the free induction decays. Chemical shift assignments were externally referenced relative to 85% orthophosphoric acid at 0.00 ppm. Abbreviations used in peak assignments: PA, phosphatidic acid; PC, phosphatidylcholine; PE, phosphatidylethanolamine; PI, phosphatidylinositol.

3. pH-dependent spectra of water-soluble SNARF

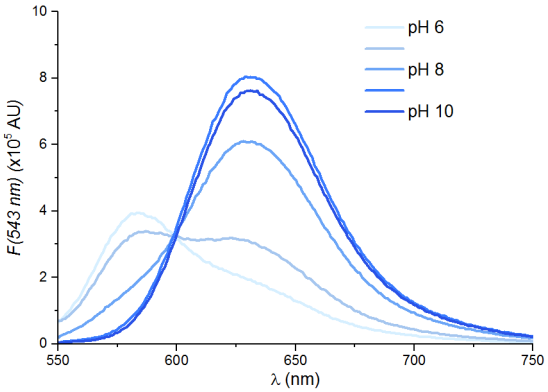

Figure S3: pH-dependent fluorescence spectra of water-soluble SNARF. Fluorescence emission spectra of water-soluble SNARF in buffer solutions of different pH upon excitation at 543 nm. All measurements were made in pH-adjusted buffers of the indicated pH values containing the protonophore CCCP (5 µM) and the K^+-ionophore valinomycin (62.5 nM). Each spectrum represents an aliquot of the water-soluble dye diluted in the respective buffer.

4. Size distribution of liposomes containing pH-sensors

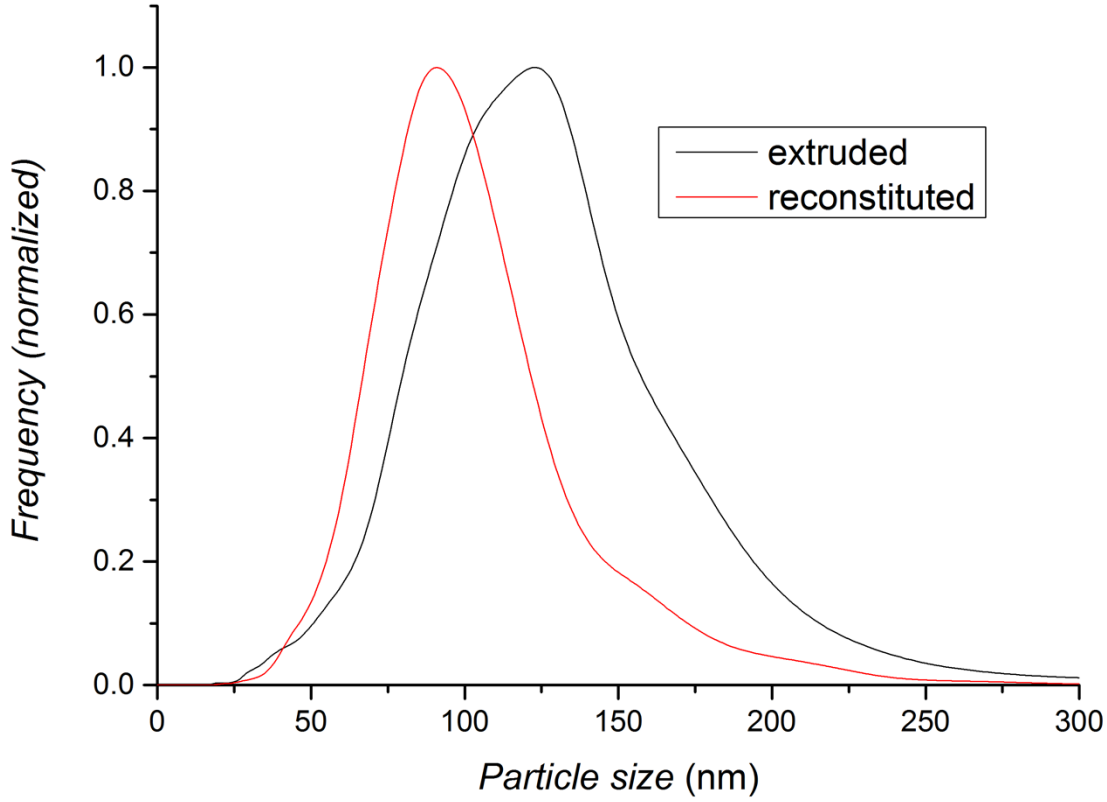

Figure S4: Size distribution for pHrodo-DOPE doped liposomes. Liposomes were formed by extrusion as described in the Experimental section and measured before (black) and after undergoing reconstitution in the presence of AHA2 (red). The size of the vesicles was characterised via nanoparticle tracking analysis (NanoSight LM14, Malvern). After liposome extrusion, the preparations exhibited mean particle diameters of 134 ± 45 nm. The size was decreased during reconstitution, resulting in proteoliposomes with a diameter of 109 ± 31 nm. Measurements were performed in triplicate at 25 °C for 90 sec, respectively. Viscosity factors for analysis were calibrated using 100 nm reference beads (polystyrene). Size distribution blots represent all measured particles for the respective condition.

5. Pyranine and pHrodo-PE fluorescence changes during H^+ pumping by reconstituted H^+-ATPase

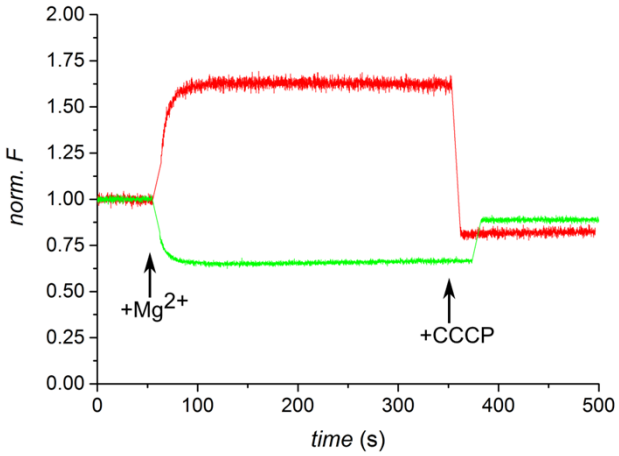

Figure S5: Time traces of proton pumping by reconstituted H+-ATPase using pHrodo-PE (red) and pyranine (green) fluorescence. Relative fluorescent changes for proteoliposomes reconstituted in presence of pHrodo-PE-doped liposomes (red) and pyranine (green). Aliquots (10 µL) of the same proteoliposomes were measured consecutively in 2 mL transport buffer (20 mM MOPS-KOH, pH 7.0, 52.5 mM K_2SO_4) containing 62.5 nM valinomycin. Addition of 3 mM Mg^{2+} to ATP-containing buffer (2 mM) initiated ATP hydrolysis and H^+ pumping into the vesicle lumen. Valinomycin was always present to mediate K^+ exchange and prevent the build-up of a transmembrane electrical potential. After reaching saturation conditions the H^+ gradient was disrupted by the addition of CCCP (5 µM final concentration). Fluorescence traces were recorded for 600 s at 25 °C by a Fluoromax-4 spectrofluorometer at the following settings: 532 nm excitation, 585 nm emission, 3 nm slit widths, 0.1 s resolution (pHrodo) and 460 nm excitation, 1 nm slit width, 515 nm emission, 2 nm slit width, 0.1 s resolution (pyranine).

6. Conversion of fluorescent intensity to pH

To calibrate fluorescence changes of pHrodo-DOPE to changes in pH, time traces were first corrected for pHrodo-DOPE in the outer monolayer of liposomes using empty liposomes.

Total fluoresence intensity (F_t) is the sum of intensities of pH-sensors residing in the inside and outside monolayer (F_i, and F_o, respectively)

$$F_t = F_i + F_o$$

Fluorescence of pHrodo-DOPE is dependent on pH, concentration of fluorophore, and its environment. Given the similarity of reconstitution and proton pumping buffer (inside respectively outside of liposomes), and the equilibration time before measurements (15-30 min), we assume the same pH and environment for both monolayers before ATP/Mg^{2+}-addition. Given the size of the liposomes, we furthermore assume an equal number of pHrodo-DOPE molecules on both leaflets. This simplifies the equation above to:

$$F_t[0] = 2F_i[0] = 2F_o[0]$$

Where $F_t[0]$ denotes total fluorescence intensity before additions, subscripts denote i, inside, and o, outside, respectively.

A stepwise fluorescence intensity decrease can be observed upon ATP-addition (data not shown), and Mg^{2+}-addition (Figure 4B, black trace, Figure 4D). Using empty liposomes, the relative change δ_1, respectively δ_2, can be quantified.

$$\delta_1 = \frac{F_t[1]}{F_t[0]}$$

$$\delta_2 = \frac{F_t[2]}{F_t[0]}$$

Where $F_t[1]$, $F_t[2]$, total fluorescence intensity after 1st addition (ATP), and 2nd addition (Mg^{2+}), respectively. For ATP- and Mg^{2+}-addition in Figure 4B, these factors were 0.928, and 0.905, respectively.

In the absence of the protein, we assume that this change in intensity can be attributed to pH-sensor molecules residing in the outer monolayer only. More precisely, we assume: (i) ATP/Mg^{2+} cannot pass the lipid bilayer to interact directly with inner monolayer pH-sensor

molecules; (ii) ATP/Mg^{2+} interaction with the outer monolayer is not coupled to the inner monolayer; (iii) liposomes are tight towards small pH-changes upon additions (ΔpH = 0.06) in the time course of the experiment. It follows:

$$F_i[0] = 0.5F_t[0] = F_i[1] = F_i[2]$$

The change in the outside monolayer pH-sensors can then be calculated as follows

$$\phi_1 = \frac{F_o[1]}{F_o[0]} = \frac{F_t[1] - F_i[0]}{0.5F_t[0]} = \frac{\delta_1 F_t[0] - 0.5F_t[0]}{0.5F_t[0]} = 2\delta_1 - 1$$

$$\phi_2 = \frac{F_o[2]}{F_o[0]} = \frac{F_t[2] - F_i[0]}{0.5F_t[0]} = \frac{\delta_2 F_t[0] - 0.5F_t[0]}{0.5F_t[0]} = 2\delta_2 - 1$$

For ATP- and Mg^{2+}-addition in Figure 4B, this yields 0.857, and 0.809, for ϕ_1, and ϕ_2, respectively.

These values can then be used to correct total fluorescence in presence of protein for the response of the outside fluorophores.

$$F_i[1] = F_t[1] - F_o[1] = F_t[1] - \phi_1 F_o[0] = F_t[1] - 0.5\phi_1 F_t[0]$$

$$F_i[2] = F_t[2] - 0.5\phi_2 F_t[0]$$

Finally, fluorescence intensity from the inside monolayer is converted to pH using the calibration curve in absence of CCCP, ATP, and Mg^{2+} (Figure S3). The parameters of the best fit to the Boltzmann function were determined as follows.

$$Norm.F(532\ nm) = \frac{A1 - A2}{1 + e^{(pH - pK_a)/dx}} + A2$$

With *A1* = 1.02617, initial value, *A2* = 0.0502, final value, pK_a = 6.05904, center, *dx* = 0.36011, slope in the center, $Norm.F(532\ nm)$, max fluorescence intensity normalized to 1 at pH 3.

Normalization was performed by dividing inside fluorescence intensities by intensities before Mg-addition and multiplying with the expected $Norm.F(532\ nm)$ at the pH measured (for red trace in Figure 4B, *pH* = 6.78, $Norm.F(532\ nm)$ = 0.166).

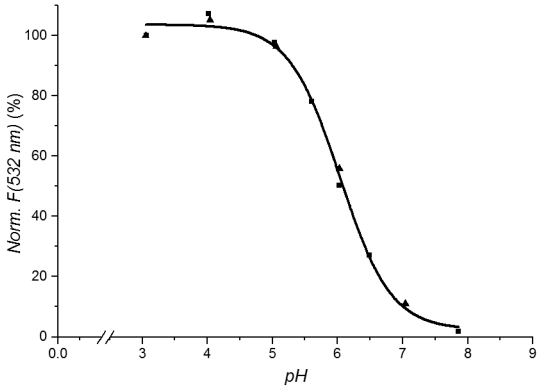

Figure S6: pH-calibration curve of vesicle-embedded pHrodo-DOPE. All measurements were performed in pH-adjusted buffers of the indicated pH values containing the K^+-ionophore valinomycin (62.5 nM). To equilibrate the pH between the inside and outside of the liposomes, an aliquot of the same liposomes was diluted in buffer and incubated for 20 h. Different symbols denote 2 independent experiments; line represents global nonlinear least squares fit to the Boltzmann function. Norm. F, max fluorescence intensity for each pH was normalized to the maximum at pH 3.

This yields normalized fluorescence values for the entire time course. These are then used to evaluate the Boltzmann function solved for pH:

$$pH = \ln\left[\frac{A1 - A2}{Norm.\,F(532\ nm) - A2} - 1\right] \cdot dx - pK_a$$

It should be noted that under conditions used here, this procedure yields lower values for *ΔpH* than assuming that half of the initial fluorescence (in presence of ATP) is contributed by fluorophores on the outside monolayer and stays constant during additions, although the difference is minor (*ΔΔpH* = 0.019) compared to the variation between experiments (*SD* = 0.16). Whether the latter, much simpler procedure can be chosen should be carefully evaluated for each experiment.